# Spatial and temporal variability of urban fluxes of methane, carbon monoxide and carbon dioxide above London, UK.

Carole Helfter[1], Anja H. Tremper[2], Christoforos H. Halios[3], Simone Kotthaus[3], Alex Bjorkegren[4], C. Sue B. Grimmond[3], Janet F. Barlow[3], Eiko Nemitz[1]

[1] Centre for Ecology and Hydrology, Penicuik, EH26 0QB, UK

[2] MRC-PHE Centre for Environment and Health, King's College London, London, SE1 9NH, UK

[3] Department of Meteorology, University of Reading, Earley Gate, PO Box 243, Reading, RG6 6BB, UK

[4] King's College London, Strand Campus, London, WC2R 2LS, UK

*Correspondence to*: Carole Helfter (caro2@ceh.ac.uk)

**Abstract.** We report on more than three years of measurements of fluxes of methane ($CH_4$), carbon monoxide (CO) and carbon dioxide ($CO_2$) taken by eddy-covariance in central London, UK. Inter-annual variability in the period 2012-2014 ranged from 36.3 to 40.7 ktons $km^{-2}$ $y^{-1}$ for $CO_2$, and from 69 to 75 tons $km^{-2}$ $y^{-1}$ for $CH_4$. Mean annual emissions of $CO_2$ (39.1 ± 2.4 ktons $km^{-2}$ $y^{-1}$) and CO (89 ± 16 tons $km^{-2}$ $y^{-1}$) were consistent (within 1% and 5% respectively) with values from the London Atmospheric Emissions Inventory, but measured $CH_4$ (72 ± 3 tons $km^{-2}$ $y^{-1}$) was over two-fold larger than the inventory value. Seasonal variability was large for CO with a winter to summer reduction of 69%. Monthly fluxes of CO were strongly anti-correlated with mean air temperature, and the winter emissions accounted for 45% of the annual budget. The winter increment in CO emissions was attributed mainly to vehicle cold starts and reduced fuel combustion efficiency. $CO_2$ fluxes were 33% higher in winter than in summer and anti-correlated with mean air temperature, albeit to a lesser extent than for CO. This was attributed to an increased demand for natural gas for heating during the winter. The seasonality in $CH_4$ fluxes was moderate (21% larger in winter) and the linear anti-correlation with air temperature was spatially-variable. Differences in resident population within the flux footprint explained up to 90% of the spatial variability of the annual $CO_2$ fluxes and up to 99% for $CH_4$.This suggests a significant influence of anthropogenic sources in the overall emissions budget of these two greenhouse gases. Furthermore, we suggest that biogenic sources of $CH_4$, such as waste water which is unaccounted for by the atmospheric emissions inventories, make a substantial contribution to the overall budget and that commuting dynamics in and out of central business districts could explain some of the spatial and temporal variability of the emissions. To our knowledge, this study is unique given the length of the datasets presented, especially for CO and $CH_4$ fluxes. This study offers an independent verification of "bottom-up" emissions inventories and demonstrates that the urban sources of CO and $CO_2$ are well characterised in London. This is however not the case for $CH_4$ emissions which are heavily-underestimated by the inventory approach. This opens up opportunities in the UK and abroad to identify and quantify the "missing" sources of urban methane,

revise the methodologies of the atmospheric inventories and devise emission reduction strategies for this potent greenhouse gas.

## 1 Introduction

The use of eddy-covariance for the measurement of turbulent fluxes of heat and mass has grown steadily over the past three decades; recently, there were > 400 active sites worldwide (Baldocchi, 2008) spanning six continents. The vast majority of existing sites were established to measure biosphere-atmosphere exchanges of carbon dioxide ($CO_2$) and heat (Baldocchi et al., 2001). Due to recent technological advances, i.e. the development of new fast response analysers, measurements of eddy-covariance fluxes of other trace gases such as methane ($CH_4$) and nitrous oxide ($N_2O$) are gradually being introduced (Crosson, 2008; Fiddler et al., 2009; Peltola et al., 2014). With the negotiation of international agreements to greatly reduce greenhouse gas (GHG) emissions by the end of the 21$^{st}$ century, there is an ever increasing need to verify emissions through independent monitoring approaches. Despite 54% of the worldwide population currently living in cities, a figure which could rise to 66% by 2050 (United Nations, 2014), and urban $CO_2$ emissions estimated to represent 70% of the global budget (International Energy Agency, 2012) there are comparatively few urban studies to evaluate reported GHG emissions. At the time of writing, 61 urban flux towers were listed in the FLUXNET Urban Flux Network database, of which 40 were located in temperate areas (Grimmond and Christen, 2012). At present, most published urban studies have focused on $CO_2$ at time scales ranging from a few months to a few years (e.g. Christen et al., 2011; Helfter et al., 2011; Pawlak et al., 2011; Jarvi et al., 2012; Liu et al., 2012). Methane, a potent GHG with a global warming potential 28 times larger than that of $CO_2$ at the 100-year horizon (IPCC, 2013), is receiving increasing attention. Whilst $CO_2$ emissions are very closely linked to fuel consumption, for which robust statistics can be obtained (at least at country level), $CH_4$ originates from a much larger range of sources with complex controls. $CH_4$ emissions are commonly estimated in "bottom-up" inventories at the national scale (e.g. for IPCC reporting), but also at the urban scale (e.g. London Atmospheric Emissions Inventory (LAEI) in the UK and the California Air Resources Board (CARB) in the USA). A variety of techniques have recently been applied to provide independent top-down estimates of urban $CH_4$ emissions. These include ground-based mass balance approaches (McKain et al., 2015), airborne observations (O'Shea et al., 2014; Cambaliza et al., 2015), Fourier Transform Spectrometry (FTS) (Wunch et al., 2009), isotopic source apportionment studies (e.g. Lowry et al., 2001; Zazzeri et al., 2015) and eddy-covariance (Gioli et al., 2012; Pawlak and Fortuniak, 2016).
We report on over three years of continuous measurements of fluxes of methane, carbon monoxide and carbon dioxide in the heart of London, UK, the largest European city. This is, to our knowledge, the longest continuous urban record of direct $CH_4$ emission flux measurements. This paper investigates the temporal and spatial emission dynamics of the three pollutants and compares annual budgets with the bottom-up emissions inventory estimates.

## 2 Materials and methods

### 2.1 Site description

Fluxes of carbon monoxide (CO), carbon dioxide ($CO_2$) and methane ($CH_4$) were measured by eddy-covariance (EC) from the rooftop of a 190 m telecommunication tower (BT tower; located at 51° 31' 17.4''N, 0° 8' 20.04''W) in central London, UK. The measurements, which are ongoing at the time of writing, began in September 2011. The period September 2011 to December 2014 is analysed here. The mean building height in a radius of ca. 10 km from the tower is 8.8 m ± 3.0 m and typically 5.6 m ± 1.8 m for suburban areas (Wood et al., 2010; Evans, 2009). The Greater London area, which extends ca. 20 km in all directions from the BT tower, has a population of 8.6 million (Mayor of London Office, 2015) and population densities in excess of $10^4$ inhabitants $km^{-2}$ in the central boroughs.

### 2.2 Instrumentation

#### 2.2.1 BT tower site

The eddy-covariance system used at the BT tower consisted of a 3D ultrasonic anemometer (R3-50, Gill Instruments), a Picarro cavity ringdown spectrometer (CRDS) model 1301-f for the measurement of $CO_2$, $CH_4$ and $H_2O$ mole fractions and an Aerolaser fast CO monitor model AL5002. The anemometer was mounted on top of a lattice tower located on the roof of the BT tower giving an effective measurement height of 190 m above street level. The two gas analysers were located a few floors below the roof, in an air conditioned room. Air was sampled from ca. 0.3 m below the anemometer head at 20-25 lpm using a 45 m long Teflon tube of OD 9.53 mm (3/8''). The Picarro CRDS was fitted with an in-house auto-calibration system and calibrated weekly using two different mixtures of methane and carbon dioxide in nitrogen (above and below typical ambient concentrations). The anemometer operated at 20 Hz, the CO analyser at 10 Hz and the Picarro CRDS, which was set to sample in 3-species mode, operated at 1 Hz. The data were captured by an in-house LabView™ (National Instruments) data acquisition program which also controlled the auto-calibration system and fluxes were processed offline by a custom LabView program. Although the Picarro 1301-f has the capability to measure concentrations at 10 Hz, at this rate, this older instrument can only measure two of the three compounds $CO_2$, $CH_4$ and $H_2O$. Because an internal $H_2O$ measurement is required for accurate corrections (e.g. Peltola et al., 2014), this would mean that in fast-response mode the instrument can only measure the flux of $CO_2$ or $CH_4$ at any one time. Due to the high measurement height, it was found that a response time of 1 Hz was sufficient to capture >70% of the flux (see below).

In addition to the closed-path system described above, an open-path infrared gas analyser (IRGA model Li7500, LI-COR Biosciences) measuring $CO_2$ and $H_2O$ at 20 Hz was mounted next to the ultrasonic anemometer on the roof of the BT tower. Both analysers used the same anemometer but data were processed independently with different eddy-covariance software packages. In what follows, subscripts "$_{CP}$" and "$_{OP}$" will respectively denote the closed-path and open-path eddy-covariance systems, and fluxes derived from them, located at the BT tower.

### 2.2.2 King's College London site

Fluxes of $CO_2$ measured by EC_CP ($F_{CO2\_CP}$) were compared to fluxes measured at an eddy-covariance site at King's College London (KCL; use of subscript "_KCL" to identify this eddy-covariance system in what follows) Strand campus, about 2 km south-east of the BT tower, where long-term EC measurements have been analysed to study energy exchanges (Kotthaus and Grimmond, 2014a, b), carbon dioxide fluxes (Ward et al., 2015) and the $F_{CO2}$ storage term in a dense urban environment (Bjorkegren et al., 2015). Carbon dioxide fluxes are obtained from observations of an open-path Li7500 gas analyser and a CSAT3 sonic anemometer (Campbell Scientific). KCL is within the flux footprint of the BT tower during south-easterly wind directions. Fluxes of $CO_2$ from the KCL site were processed as outlined by Kotthaus and Grimmond (2014a).

For the time August – September 2015, a methane sensor (Aerodyne Quantum Cascade Laser (QCL)) was added to the EC system at KCL to also observe $F_{CH4}$. No carbon monoxide was measured at KCL. The EC_KCL system was operated at the top of a tower situated on the roof of a large building resulting in a measurement height of 50 m above mean ground level in the flux footprint (Ward et al., 2015), i.e. ca. 140 m lower than for EC_CP. Given that the KCL site is closer to the urban canopy, the source area extends to several hundred metres, while the footprint of the BT tower is much larger, i.e. in the order of kilometres. The QCL measured methane, nitrous oxide ($N_2O$) and water vapour simultaneously and at 10 Hz. The instrument was housed in an air-conditioned cabinet to minimise temperature fluctuations. Air was sampled ca. 20 cm below the anemometer head at 20 lpm through a 25 m long Teflon tube with outer diameter 1.27 cm (1/2''). The data was logged using an in-house LabView program and processed offline as outlined in section 2.3.

## 2.3 Data processing and filtering

Half-hourly fluxes were calculated using standard eddy-covariance methodology extensively described elsewhere (e.g. Aubinet et al., 2000; Foken et al., 2004; Moncrieff et al., 2004). The quality control procedures and the performance of the eddy-covariance system at the tall tower are presented in sections 2.3.1 to 2.3.3.

### 2.3.1 High frequency attenuation

Normalised cospectra ('Co(x)') of $wCO_2$ and $wCH_4$ measured by the closed-path system were corrected to match those of wT (where T is sonic temperature) to assess high frequency damping caused by the instrument's limited sampling rate (1 Hz), internal instrument time response and the long inlet line (~ 45 m). Co(wT) followed the theoretical $f^{-5/3}$ (where f denotes frequency) slope for the inertial sub-range (Foken, 2008) over the entire frequency range (Fig. 2). In contrast, Co($wCO_2$) and Co($wCH_4$) diverged from the theoretical slope for frequencies > 0.1 Hz and followed profiles with slopes of the order of ~ $f^{-5/2}$. Relative humidity did not have a significant influence on Co($wCO_2$) and Co($wCH_4$) for the two regimes tested (RH = 52% and RH = 80%, data not shown) which suggests that the dominant causes of signal attenuation for our system were the sampling rate and the length of the inlet line. Typical corrections for high frequency attenuation ranged from 15%-30% and based on the co-spectra presented in Fig. 2 it can be inferred that eddies of frequency < 0.1 Hz carried > 70% of the flux measured at the 190 m above-street-level sampling height. The net flux loss resulting from high frequency attenuation was of the order of

30% over the entire frequency range. Each half-hourly flux was corrected for high frequency attenuation as part of the offline data processing procedure on a point per point basis.

### 2.3.2 Quality control and filtering

Half-hourly means were excluded if any of the following quality assurance criteria were not fulfilled:

- The number of raw data points per nominal half hour was < 35000.
- The flow rate in the sampling line was less than 15 lpm (theoretical limit of the transitional phase between laminar and turbulent flow for the sampling tube diameter used in this study).
- The number of spikes in u, v, w (components of the 3D wind vector measured by the ultrasonic anemometer) or any of the trace gas mole fractions was > 360 (i.e. 1% threshold).
- Latent and sensible heat fluxes fell outside the -250 W $m^{-2}$ to +800 W $m^{-2}$ range.
- The level of turbulence was deemed insufficient for flux measurement (friction velocity, $u_*$, threshold of 0.2 m $s^{-1}$). This threshold was used for consistency with previous studies carried out at the BT site (Helfter et al., 2011; Langford et al., 2010).
- The stationarity test which requires that the difference between the half-hourly flux and the fluxes obtained from 6 x 5 min averaging sub-intervals does not exceed 30% is satisfied (Foken and Wichura, 1996; Foken, 2004).

### 2.3.3 Comparison between closed-path and open-path systems

The performance of the closed-path greenhouse gas eddy-covariance system located on the 35$^{th}$ floor of the BT tower ($EC_{\_CP}$) was compared to that of the open-path IRGA located on the roof of the tower ($EC_{\_OP}$). $EC_{\_CP}$ operated at 1 Hz, $EC_{\_OP}$ at 20 Hz and.

After frequency correction, half-hourly $CO_2$ fluxes measured by an open-path Li7500 infrared gas analyser located on the roof of the BT tower ($F_{CO2\_OP}$) were strongly correlated to the fluxes obtained with the closed-path Picarro analyser ($F_{CO2\_CP}$; Fig. 3). Increased scatter in $F_{CO2\_CP}$, especially during low fluxes, could be due to uncertainties in determining the time-lag through maximisation of the covariance or also to uncertainties arising from the open-path analyser. The slope of near unity indicates that the high frequency attenuation of the turbulent flow due to instrument response time, sampling flow rate and length of the sampling line was adequately and systematically corrected for.

$F_{CO2\_CP}$ clearly varied with friction velocity ($u_*$) with maximum fluxes observed at $u_*$ values around 0.8 m $s^{-1}$, strongly reduced fluxes at low $u_*$ < 0.3 m $s^{-1}$ and the indication of reduced values at very high values of $u_*$ (Fig. S2). A similar $u_*$ dependence was found for the fluxes from the open-path gas analyser (not shown). Near-zero fluxes were recorded by both systems for $u_*$ values < 0.1 m $s^{-1}$. For $CO_2$ flux measurements over vegetation, this type of behaviour is usually attributed to a reduction in

the transport to the measurement height, resulting in storage of $CO_2$ below that height which may be subject to advection. In the urban environment, this $u_*$ dependence could alternatively arise from an actual correlation between $u_*$ and surface emission. Indeed, on average both $u_*$ and traffic counts show a minimum at night. However, it is likely that a loss of coupling with street level sources as a result of limited vertical transport occurred in situations of low turbulence. These situations often coincide with stable night-time conditions during which the boundary layer height can approach that of the measurement height (Barlow et al., 2015). In such conditions the measured flux would be an underestimate of the true surface emission due to change in storage in the air column below the measurement height. An explicit treatment of the storage term based on a gradient approach where concentrations and wind speeds are recorded at multiple heights below the EC measurement point could help probe the low $u_*$ regime. Such additional measurements were however not available for the BT tower site and we therefore speculate that the observation of venting after onset of turbulence, when the boundary layer grows, would capture at least some if not most of the material stored below the measurement height.

### 2.4 Uncertainty analysis

Random measurement uncertainties were estimated for each half-hourly averaging period using the Finkelstein and Sims (2001) method and subsequently averaged into monthly means. The upper bounds of the random uncertainties associated with the annual emissions estimates were taken as the maximum monthly random uncertainty for each year and trace gas.

Unlike random uncertainties, which arise from instrument noise and representativeness of single-point measurements, systematic errors can be minimised by careful data processing and correction. In particular, successive calibration events were linearly interpolated over time, cancelling out errors due to calibration drifts assuming that the drift was linear over time.

So far we have considered the error in the local flux. In addition, there is an uncertainty of how this local flux relates to the emission at the surface. The effects of advection and storage on the flux measurement are difficult to quantify in a heterogeneous environment like a city. However, whilst individual half-hourly flux values may be a poor representation of the momentary emission, we expect the errors to reduce significantly when long-term averages are analysed. The validity of this assumption is explored in more detail in what follows.

## 3 Results and discussion

### 3.1 Flux footprint

For consistency with a previous study (Helfter et al., 2011), the flux footprint for the BT tower measurement site was estimated with the analytical model of Kormann and Meixner (2001) for non-neutral atmospheric stratification, under the simplifying assumptions that fluxes of heat and momentum were homogenous across the footprint. The frequency of observation of $x_{90}$, the distance from the tower where 90% of the measured fluxes originated from, is shown in Fig. 1 as a function of wind

direction and season for the measurement period 2011-2014. The spatial extent of the flux footprint was highly variable over time with recurring seasonal patterns. Typically, 90% of the flux measured at the BT tower site originated from distances of the order of a few km in spring and summer compared to several tens of km in winter. The flux footprint contains two large parks in the SW (Hyde Park, surface area 142 ha) and NW (Regent's Park, surface area 197 ha), sub-urban residential areas in the N, a mixture of heavily urbanised residential and commercial areas in the E and S and a section of the Thames river in the SE.

### 3.2 Comparison with flux measurements at a lower height

#### 3.2.1 Temporal similarities

$F_{CO2\_CP}$ and $CO_2$ fluxes observed at the KCL site ($F_{CO2\_KCL}$) exhibited a high temporal correlation for diurnal patterns in both winter and summer (Fig. 4a, b; averaging period 15/09/2011 to 31/12/2013). Daily minima occurred at around 3:00 at both sites which is consistent with minimum traffic loads (Fig. 4f, g). Fluxes tended to increase from ca. 5:00-6:00 until late morning and declined steadily from ca. 18:00 at both sites, which is again in agreement with the declining traffic numbers in the evening. Methane fluxes exhibited similar temporal dynamics with the lowest emissions recorded during the night and a sharp rise between ca. 5:00 and 8:00. A gradual decrease in $F_{CH4}$ was observed at both sites following the mid-morning maximum.

In winter, carbon dioxide fluxes started to increase slightly earlier (by about 30 min on average) at the KCL site. While this time lag was not evident in the summer for $F_{CO2}$, methane fluxes started rising later at the elevated measurement point at BT tower even in summer. Boundary layer growth in the morning transition period might explain some of the time delay observed in the carbon fluxes. Mixing height (MH) estimates for several weeks in winter (6 Jan – 11 Feb 2012) and summer (23 July – 17 Aug 2012) derived from Doppler LIDAR turbulence measurements (Bohnenstengel et al., 2015) at sites close to BT tower (Fig. 4d, e) indicate that, on average, turbulent mixing extended above the BT tower measurement height of 190 m in both seasons. However, mixing height exhibits great temporal variability depending on the synoptic background conditions; for London it has been found that MH development depends primarily on the boundary layer winds and stability (Halios and Barlow, 2016) so that these short-term climatology estimates might not be representative for the full period analysed for the turbulent fluxes.

Growth of the convective layer was rapid in summer and a plateau was typically reached mid-morning which lasted until late afternoon. In agreement with the shorter day-length in winter, growth of the mixing height was slower, collapsing earlier in the evening after the mid-afternoon maximum. Daytime maximum mixing height was about 30% lower in winter compared to the summer. In both summer and winter, traffic counts rose during the morning transition period i.e. before the mixing layer started growing considerably (Fig. 4f, g); in the evening, traffic counts began decreasing after the mixing height had reduced in height. Given that the mean temporal evolution of carbon dioxide fluxes observed at both KCL and BT tower appeared to be closely linked to the profiles of road traffic, vehicle emissions apparently represent a significant control not only for the local-scale observations at KCL (Ward et al., 2015) but also for fluxes at the elevated BT tower measurement point (Helfter et al., 2011). The slight morning delay in wintertime $F_{CO2}$ (Fig. 4a) observed at BT tower might be explained by the efficacy of

vertical turbulent transport between street level and the top of the BT tower which has been shown to depend on atmospheric stability. The timescale of upward vertical turbulent transport was estimated to be of the order of 10 minutes for near-neutral conditions, increasing to 20-50 minutes for stable conditions (Barlow et al., 2011). Low turbulence and prolonged periods of stable atmospheric stratification (Fig. S3) could thus explain the 1-2 hour lag between the timing of the morning increase in traffic counts and fluxes of $CO_2$ at the BT tower during the winter (Fig. 4a). This is consistent with the lag time observed for profiles of potential temperature, and thus upward mixing, measured at the BT tower and a lower-level measurement site close to the BT tower at 18 m a.g.l. (Barlow et al., 2015). The near-synchronous rise in $CO_2$ and $CH_4$ fluxes observed in summer (summer defined as the months (JJA) in the data period 15/09/2011 - 31/12/2013 for $F_{CO2}$ and the entire period 19/08 – 01/10/2015 for $F_{CH4}$) at the two measurement sites (BT and KCL) at different heights is consistent with an earlier onset of turbulent mixing (Fig. 4 b,c).

Storage fluxes are difficult to quantify accurately in a heterogeneous environment like a city as this would require vertical profile measurements below the measurement height at several locations within the flux footprint. The analysis presented here therefore relies to some extent on the assumption that, over long periods, positive and negative storage fluxes cancel out and that effects of advection on the stored quantity are negligible. This assumption is further supported by the very small storage fluxes (< 2.5 % of the magnitude of the vertical fluxes) calculated at the KCL site (Bjorkegren et al., 2015), although these would be somewhat larger for the higher measurement height at BT. While the turbulent fluxes observed at the BT tower and KCL show close temporal alignment (Fig. 4a-c) their absolute values can differ considerably (e.g. KCL-to-BT ratios of peak $FCO_2$ ranged from 1.5 in winter to 0.9 in summer; the summer ratio for $FCH_4$ was 1.5).

### 3.2.2 Comparison of flux spatial variability at the elevated and roof-top sites

Both sites are situated in central London where anthropogenic emissions are high due to the elevated density of people and traffic (Ward et al., 2015). While the source area of the BT site includes central business district (CBD) areas with mostly medium density midrise building structures, residential areas as well as large parks, the KCL footprint is dominated by CBD structures with hardly any vegetation (Kotthaus and Grimmond, 2014b). Only the river Thames in its vicinity reduces anthropogenic emission in some parts of the KCL footprint. To evaluate the response of $F_{CO2\_CP}$ and $F_{CO2\_KCL}$ to variations in source area characteristics, the observations were grouped into eight sectors based on the wind direction measured at the BT tower (Fig. 5). The carbon dioxide fluxes observed at the two sites are linearly correlated for all eight wind sectors but slope and goodness of fit vary. This is likely due to differences in flux footprints at the two measurement sites, including the extent (a few km at the BT tower and a few hundred metres at KCL; Kotthaus and Grimmond, 2014b) as well as emission source density (a function of surface types). Near 1:1 agreement was found in the dominant SW wind sector (Fig. 5). For other wind directions, differences in local-scale source area between the two EC sites become apparent: while a large green space (Regent's Park) is located to the NW of BT tower, the surface seen by the KCL measurements is least urbanised towards the S and SE of the site (river Thames; note that busy Waterloo bridge towards the SW of KCL acts as a very strong line source of $CO_2$ keeping the fluxes relatively high from this wind direction). In response to the surface cover, $F_{CO2\_CP}$ exceeds $F_{CO2\_KCL}$

in the E, S and SE wind sectors by 20%, 50% and 70%, respectively, and is lower by 50%-70% in the N, NW and W sectors with the poorest correlation for the NW sector. The smallest $F_{CO2\_CP}$ fluxes were observed in the NW sector while $F_{CO2\_KCL}$ was highest in sectors NW and W where the particularly busy Aldwych junction is located (Kotthaus and Grimmond, 2014a). KCL falls within the footprint of the BT tower site for SE wind direction, but clearly the BT tower measurement sees additional sources due to the larger footprint. The focus was placed on discussing $CO_2$ fluxes in this section is because it is the only compound for which we have a second long-term flux record at a lower measurement height. However, we assume that all the conclusions (pertaining to e.g. spectral corrections, turbulent transport) in this section are also applicable to $CH_4$ and CO.

### 3.3 Diurnal variability of the measured fluxes

The fluxes of all three gases ($F_{CO}$, $F_{CO2}$ and $F_{CH4}$) exhibited well-defined diurnal cycles with minimum emissions during the night, typically from midnight until 5:00 GMT (Fig. 6a-c). Emissions increased sharply from 6:00 reaching a daytime maximum at around 12:00, and then declined steadily until early evening when a local maximum was observed at around 18:00-19:00. Mean $F_{CH4}$ ranged from 5.7 to 11.0 kg km$^{-2}$ hour$^{-1}$ (maximum-to-minimum ratio of 1.9), $F_{CO2}$ from 1867 to 6635 kg km$^{-2}$ hour$^{-1}$ (maximum-to-minimum ratio 3.5) and $F_{CO}$ from 4.6 to 16.9 kg km$^{-2}$ hour$^{-1}$ (maximum-to-minimum ratio 3.7), demonstrating that the relative dynamic range of $F_{CH4}$ is less than that of the other compounds.

Urban $CH_4$ emissions from developed cities are thought to be dominated by leakage from the natural gas distribution network and this is also reflected in the source sector breakdown of the LAEI. Assuming that constant pressure is maintained throughout the gas distribution network, the leak rate should be constant through the day. Thus, Gioli et al. (2012) interpreted non-negligible diurnal cycles in $F_{CH4}$ observed in Florence (Italy) to be caused by vertical transport following the diurnal cycle of convective mixing. This argument does not seem relevant for the present study because the diurnal variations in $F_{CH4}$ measured at the BT tower were mirrored by strongly suppressed night-time $CH_4$ fluxes observed at a much lower height at the KCL site (Fig. 4c), where the storage error has been demonstrated to be small for $CO_2$ (Bjorkegren et al., 2015). Summer time fluxes of $CH_4$ measured at the 190 m height did lag slightly behind the fluxes observed at the 50 m height, but this apparent delay could have been caused by differences in flux footprint between the sites (e.g. the source area of the BT tower fluxes has a much higher fraction of vegetation cover than the KCL footprint) and the fact that the diurnal profiles were obtained for a much shorter time period (August-September 2015). Instead, the similarity in $F_{CH4}$ temporal dynamics between the two sites supports the idea that the diurnal variations for that gas represent real variability in its source strength rather than an artefact of atmospheric transport. This suggests that either the gas supply pressure in the distribution network exhibits diurnal variations and/or that other $CH_4$ sources with temporal variations are more significant than estimated by LAEI. This is further supported by $F_{CH4}$ being smaller at the weekend than on weekdays (Fig. 6g).

#### 3.3.1 Dependence of flux magnitude and diurnal patterns on wind sector

Segregating emissions by wind direction reveals heterogeneous source distributions at the BT tower site with different temporal patterns (Fig. 6d-f) and source strengths (Fig. S4-S6). The lowest emissions (± standard error of the mean) for all three

pollutants were recorded for NW winds ($F_{CO}$ = 1.7 ± 0.3 kg km$^{-2}$ hour$^{-1}$, $F_{CO2}$ = 728 ± 127 kg km$^{-2}$ hour$^{-1}$, $F_{CH4}$ = 1.9 ± 0.2 kg km$^{-2}$ hour$^{-1}$). The highest emissions of methane were found in the SE wind sector (17.8 ± 1.3 kg km$^{-2}$ hour$^{-1}$), in the S sector for carbon dioxide (9020 ± 515 kg km$^{-2}$ hour$^{-1}$) and in the E sector for carbon monoxide (25.4 ± 3.9 kg km$^{-2}$ hour$^{-1}$). The difference in emissions between wind sectors was however only statistically significant for the N and NW wind sectors. Maxima of $F_{CO}$, $F_{CO2}$ and $F_{CH4}$ occurred on average at around 7:00-8:00 in the NW sector. Peak emissions for $F_{CO2}$ and $F_{CH4}$ in the remaining wind sectors occurred typically between 9:00 and 12:00. The overall diurnal profile of $F_{CO}$ was bimodal, except for NE and NW, with well-defined mid- to late-morning peaks (typically 9:00 to 12:00 GMT) followed by early evening peaks (17:00 to 19:00). $F_{CO}$ and $F_{CO2}$ reached night time minima at around 3:00 in all wind sectors whereas $F_{CH4}$ tended to plateau, except in the SE where emissions tended to increase. The onset of an early morning increase in emissions (ca. 5:00-6:00 GMT) was consistent for all wind directions for $F_{CO2}$ and $F_{CO}$ but it was less clearly defined for $F_{CH4}$. In addition to diurnal trends and dependency on wind sector, emissions of all three pollutants were found to be lower on weekends (Fig. 6g-i), with $CH_4$ again showing the lowest variability (9% reduction on weekends compared to working days for $F_{CH4}$, 22% for $F_{CO2}$ and 23% for $F_{CO}$).

### 3.4 Seasonality of the measured fluxes

For the measurement period September 2011 to December 2014, $F_{CH4}$, $F_{CO2}$ and $F_{CO}$ exhibited marked seasonal cycles with minimum emissions in summer (Fig. 7a-c). The lowest emissions of CO were observed in April but this is thought to be an artefact caused by relatively low temporal and spatial coverage for that month resulting from instrument downtime. Whilst not used in the discussion that follows, the April data point is included in Fig. 7 c and f for consistency. For the months December-February, $F_{CO2}$ and $F_{CH4}$ were 4.1 ± 0.5 ktons km$^{-2}$ month$^{-1}$ and 7.4 ± 0.8 tons km$^{-2}$ month$^{-1}$, respectively, and decreased to 2.7 ± 0.3 ktons km$^{-2}$ month$^{-1}$ (33% reduction) and 5.8 ± 0.4 tons km$^{-2}$ month$^{-1}$ (21% reduction), respectively, in summer (June-August). The difference between winter and summertime emissions of carbon monoxide was 3-fold with 9.1 ± 2.5 tons km$^{-2}$ month$^{-1}$ in December-February and 2.9 ± 0.1 tons km$^{-2}$ month$^{-1}$ in June-July (due to instrument downtime, no data are available for August).

#### 3.4.1 Seasonal controls of fluxes of carbon monoxide and carbon dioxide

It is well established that emissions of CO from petrol cars are temperature dependent, e.g. increasing by a factor of 5-6 at ambient temperature 0 °C compared to 25 °C (Andrews, 2004) during the first 5-10 minutes following engine warm-up. The strong negative linear dependence of $F_{CO}$ upon air temperature (Fig. 7f) could thus indicate that cold starts and reduced combustion efficiency played an important role during winter. Winter time (December-February) emissions of CO accounted for 45% of the annual budget for this pollutant which is consistent with LAEI (LAEI, 2010) estimates of the combined natural gas and cold start contribution to annual CO emissions (total 32%, with 26% and 6% attributed to cold starts and natural gas consumption, respectively). $F_{CO2}$ was also correlated with air temperature (Fig. 7e; $R^2$ = 0.59), albeit to a lesser extent than $F_{CO}$, which reflected the seasonal changes in domestic and commercial natural gas usage, but may also be influenced by

increased photosynthetic uptake by vegetation in the footprint during the warmer months. Anti-correlations between monthly $F_{CO2}$ and air temperature have been reported in other studies (e.g. Beijing, Liu et al., 2012; London, Ward et al., 2015). The gradient between $F_{CO2}$ and air temperature observed in this study (-0.94 μmol $m^{-2}$ $s^{-1}$ °$C^{-1}$) falls between the values reported for the London site (-1.95 μmol $m^{-2}$ $s^{-1}$ °$C^{-1}$) and the Beijing site (-0.34 μmol $m^{-2}$ $s^{-1}$ °$C^{-1}$).

The flux ratio of CO to $CO_2$ is of the order of 4 mmol $mol^{-1}$ in winter (excess CO due to cold starts and incomplete combustion) and 2 mmol $mol^{-1}$ in summer despite only moderate seasonal variations in traffic loads (Fig. S7). Traffic loads at Marylebone Road, one of the busiest arteries in central London located < 1 km north of the BT Tower, varied by less than 5% seasonally in the period June 2012 to December 2014 (source Transport for London; personal communication). The seasonality of $F_{CO2}$ is hence likely controlled by changes in natural gas consumption and vegetation (Gioli et al., 2012; Helfter et al., 2011). This is further supported by relatively constant ratios of $F_{CH4}$ to $F_{CO2}$ which suggests that seasonal variations in emissions were of comparable magnitude for these two gases (Fig. S7). On average over the full three years of the study (2012-2014), summertime $F_{CO2}$ were 30% lower than in winter (29% in 2012, 30% in 2013 and 2014). In comparison, during an earlier study at the same site covering the year 2007, the winter to summer decrement was only 20% (Helfter et al., 2011).

### 3.4.2 Seasonal controls of methane emissions

Fluxes of $CH_4$ were 17% lower in summer than in winter (18%, 12% and 20% for 2012, 2013 and 2014 respectively) and the linear correlation of monthly averages with temperature was not statistically significant (Fig. 7d; $R^2 = 0.31$, p-value = 0.06). In contrast, the winter to summer decrease was of the order of 63% in the city of Łódź, Poland (Pawlak and Fortuniak, 2016) and the dependence of $F_{CH4}$ upon air temperature was statistically significant. The weaker correlation of $F_{CH4}$ with air temperature in London suggests that the total methane flux is due to a superposition of sources with constant and time-varying emission rates, whereas in Florence (Italy) no significant seasonality in $CH_4$ emissions was observed (Gioli et al., 2012). They related this to a constant pressure in the gas distribution network serving Florence. However, seasonality in both methane concentrations and methane isotopic signature have been reported in the Greater London area (Lowry et al., 2001). The winter time increase above background in $CH_4$ concentrations and the accompanying enrichment in $\delta^{13}C$ were consistent with North Sea natural gas and attributed to losses of $CH_4$ from over-pressurised pipelines in response to (or anticipation of) an increase in demand and to incomplete combustion upon boiler ignition. The seasonality of $F_{CH4}$ in Łódź (Poland) was also attributed to variations in natural gas usage (Pawlak and Fortuniak, 2016). Urban $CH_4$ emissions in Boston (USA) attributed to natural gas use also displayed a modest, albeit not statistically significant, seasonality, with lower emissions during the summer (McKain et al., 2015). An increase of total $CH_4$ emissions in summer could indicate temperature-sensitive biogenic sources played an important role in Boston. Although individually small, passive fugitive post-meter emissions (i.e. in homes or work place) can make a non-negligible cumulative contribution at the city scale (Wennberg et al., 2012). If post-meter emissions are constant in time, they would be part of the baseline $CH_4$ rather than being seasonally variable. Finally, methane emissions from liquefied petroleum gas (LPG) vehicles, although small compared to natural gas emissions, exhibit a positive dependence upon

temperature (Nam et al., 2004) and are expected to also contribute to the seasonality and diurnal variation of the total urban $CH_4$ fluxes.

### 3.5 Annual budgets of methane, carbon monoxide and carbon dioxide emissions

Annual emissions of $CO_2$ ranged from 36.3 to 40.7 ktons $km^{-2}$ $y^{-1}$ with a 3-year mean of 39.1 ± 2.4 ktons $km^{-2}$ $y^{-1}$ (Table 1). These values are in good agreement with results from a previous measurement campaign at the BT tower in 2007 (35.5 ktons $km^{-2}$ $y^{-1}$; Helfter et al., 2011) and London Atmospheric Emissions Inventory (LAEI) bottom-up emission estimates for the central London boroughs of Westminster and Camden, which are the foremost spatial source areas entrained by the BT tower flux footprint. The good agreement for $CO_2$ obtained in the present and previous studies using different instrumentation provides a benchmark for subsequent comparisons between top-down measurements and bottom-up inventory estimates. Due to insufficient temporal coverage, individual annual budgets for 2012-2014 could not be derived for carbon monoxide. Instead, one single annual CO flux value was calculated from individual monthly averages collected in the period September 2011 – December 2014 on the assumption that year-on-year variability was small. Furthermore, emissions of CO for August and September, when no observations were available, were estimated from a linear relation between $F_{CO}$ and air temperature (Fig. 7f). The composite annual emissions estimate of 89 ± 16 t $km^{-2}$ $y^{-1}$ (range taken as the random uncertainty) is consistent with the LAEI data (Table 1). Flux ratios are less sensitive to limitations in vertical transport and provide an additional means of assessing the quality of the bottom-up emission inventories and identifying poorly represented sources. Measured flux ratios of $F_{CO}$ to $F_{CO2}$ were consistent with average LAEI emission ratios (Table 2, Fig. S9). Measured flux ratios of $F_{CO}$ to $F_{CH4}$ were about half the inventoried values and measured ratios of $F_{CH4}$ to $F_{CO2}$ were twice the mean LAEI values (Table 2; Fig. S8), consistent with the measured annual $CH_4$ fluxes (3-year mean 72 ± 3 t $km^{-2}$ $y^{-1}$) being more than twice the inventory value. This indicates that some $CH_4$ sources were either underestimated or unaccounted for by the LAEI. Of the source categories included in the LAEI and listed in Table 2 only gas leakage has the potential to increase the $CH_4/CO_2$ flux ratio, but an underestimation in leakage is only a possible explanation if it follows the measured diurnal cycle, either due to changes in the supply pressure or in post-meter emissions. We speculate that the diurnal, seasonal and spatial variations in $F_{CH4}$, and the larger $F_{CH4}/F_{CO2}$ ratio could be due a contribution of temperature-sensitive $CH_4$ emissions perhaps of biogenic origin (e.g. increased methanogenesis from sewerage) not included in the inventories. This could explain why the net seasonal decrease in $CH_4$ was but half that of $CO_2$ (Fig. 7a and b). Previously reported discrepancies of 1.5 to > 2 between top-down and bottom-up estimates of $CH_4$ for the South Coast Air Basin in the greater Los Angeles (USA) area have been related to emissions from landfills and other biogenic sources (Hsu et al., 2010; Wunch et al., 2009). In our study, annual methane fluxes exhibited substantial spatial variability when segregated by wind sector (Fig. 8a). Fluxes of methane in the E, S and SE sectors were ca. 30% larger than the mean annual $F_{CH4}$ estimate and exceeded the top boundary of the overall mean (taken as mean $F_{CH4}$ + maximum monthly uncertainty; Fig. 8a). In contrast, $F_{CH4}$ from the N and NW sectors were 40% and 30% of the mean value, respectively, and fell below the lower limit of the overall mean (taken as mean $F_{CH4}$ – maximum monthly uncertainty). This perhaps suggests more complex, spatially discrete, source distribution and composition for $CH_4$ compared with $CO_2$ and CO. The linear

correlation between $F_{CH4}$ and population was strong if the highest emitting wind sectors (E, S and SE) were excluded from the regression (Fig. 8b). Socio-economic temporal dynamics, such as a significant daytime influx of commuters into a business district (e.g. the City of London financial district which is located 3-4 km S-SE of the BT tower), might contribute substantially to $CH_4$ emissions (e.g. from sewage, natural gas); in addition, the measured $CH_4$ emissions from such business areas might bear no correlation with the actual resident population reported here (source: London Datastore, Greater London Authority, 2016) which can be considerably smaller than the commuting workforce. Emissions of $CH_4$ in the E were strongly correlated with air temperature (Table 3), which suggests one or more dominant seasonal source in that wind sector. Finally, neither test was statistically significant for emissions in the SE and S where the flux footprints entrain some of the most heavily urbanised areas of central London as well as part of the river Thames. Further work is needed to investigate the potential presence of additional sources of methane which might be prevalent in those wind sectors.

As for $CH_4$, $CO_2$ fluxes exhibited a dependence upon air temperature in the N, NE, E and W. The seasonality of the $CO_2$ emissions was not statistically significant in the remaining wind sectors which might be due to the presence of substantial constant sources of $CO_2$ or to the prevalence of seasonal activities which do not emit $CO_2$ locally (e.g. more electrical heating than natural gas). However, the spatial variability of $F_{CO2}$ was well-captured by differences in population in the respective flux footprints of all wind sectors, except S (Fig. 8b).

## 4 Conclusions

This study presents the results of more than three years of continuous long-term eddy-covariance observations of fluxes of carbon monoxide, carbon dioxide and methane at an elevated measurement site (BT tower, 190 m a.g.l.) in central London, UK. This unique vantage point, combined with the length of the study, allowed for the spatial and temporal emission dynamics to be analysed in detail. The main conclusions are that all three trace gases exhibited diurnal cycles consistent with anthropogenic activities (traffic, natural gas use) and underwent marked seasonal dynamics, with reduced emissions in the summer.

*Seasonality of the measured fluxes*

Emissions of CO were strongly correlated with air temperature which is thought to be due to cold starts and reduced fuel combustion efficiency by the London fleet during the winter. Winter time emissions of CO accounted for 45% of the annual budget. Emissions of $CO_2$ were also correlated to air temperature and were 33% larger in winter than in summer. $CO_2$ emissions were predominantly controlled by the seasonal increase in natural gas consumption, although vegetation uptake would also have lowered $CO_2$ fluxes in summer. $CH_4$ fluxes averaged over all wind sectors decreased by 21% between winter and summer but unlike CO and $CO_2$, the correlation with air temperature was not statistically significant. . When segregated by wind sector, $CH_4$ fluxes in the E and W were strongly correlated with air temperature suggestive of sources with highly seasonal emission rates, possibly leaks from the natural gas distribution network or emissions from sewage. Furthermore, $CO_2$ and $CH_4$ fluxes

were positively correlated with population density in all wind sectors except S for $F_{CO2}$ and S, SE and E for $F_{CH4}$. This indicates heterogeneous source distributions and/or densities with temporal dynamics which differ from the other wind sectors.

*Comparisons with atmospheric emissions inventories*

Measured annual emissions of $CO_2$ (39 ktons $km^{-2}$) were in good agreement with bottom-up estimates from the London Atmospheric Emissions Inventory (LAEI). As $CO_2$ is the most accurately represented of the three compounds in emission inventories, this provides confidence in the flux measurements. Similarly, the measured annual budget for CO (89 tons $km^{-2}$) was consisting with LAEI values which confirms that the spatial distribution of the sources of this pollutant is well captured by the inventory. However, the measured annual $CH_4$ emissions (72 tons $km^{-2}$) were more than double the LAEI value suggesting that sources are not as well-characterised by the inventory. In particular, we hypothesise that the shortfall in inventoried $CH_4$ emissions can be explained by the existence of temperature-dependent sources, perhaps of biogenic origin (e.g. sewage).

**Acknowledgements**

The authors acknowledge a succession of projects for funding this research (NERC-funded projects ClearfLo (H003231/1), GAUGE (NE/K002279/1)) as well as support by NERC National Capability funding, the EU FP7 Infrastructure Project InGOS project (284274), the EU FP7 Grant BRIDGE (211345), and King's College London.

The authors also acknowledge British Telecom (BT) for granting use of the tall tower for research purposes. In particular, we are grateful to Karen Ahern for arranging work permits and facilitating access to the site. Thank you also to aerial riggers Robert Semon, Wayne Loeber and Mark West for help with the installation and maintenance of the rooftop instruments. We are grateful to BT security and facilities staff for their continued support and assistance with day-to-day logistics and to Dr Neil Mullinger (Centre for Ecology and Hydrology) for help with instrument maintenance and visits to the site. Supporting the KCL observations, we thank Dr Arnold Moene at Wageningen University for providing the ECpack software; all staff and students at KCL and University of Reading (Grimmond group) who contributed to the data collection; KCL Directorate of Estates and Facilities for giving us the opportunity to operate the various measurement sites.

## References


Andrews, G. E., Zhu, G., Li, H., Simpson, A., Wylie, J.A., Bell, M. and Tate, J. : The effect of ambient temperature on cold start urban traffic emissions for a real world SI car, Proceedings of SAE 2004 Powertrain & Fluid Systems Conference and Exhibition Tampa, FL, USA, October 2004, 2004.

Aubinet, M., Grelle, A., Ibrom, A., Rannik, U., Moncrieff, J., Foken, T., Kowalski, A. S., Martin, P. H., Berbigier, P., Bernhofer, C., Clement, R., Elbers, J., Granier, A., Grunwald, T., Morgenstern, K., Pilegaard, K., Rebmann, C., Snijders, W., Valentini, R., and Vesala, T.: Estimates of the annual net carbon and water exchange of forests: The EUROFLUX methodology, Advances in Ecological Research, Vol 30, 30, 113-175, 2000.

Baldocchi, D., Falge, E., Gu, L. H., Olson, R., Hollinger, D., Running, S., Anthoni, P., Bernhofer, C., Davis, K., Evans, R., Fuentes, J., Goldstein, A., Katul, G., Law, B., Lee, X. H., Malhi, Y., Meyers, T., Munger, W., Oechel, W., U, K. T. P., Pilegaard, K., Schmid, H. P., Valentini, R., Verma, S., Vesala, T., Wilson, K., and Wofsy, S.: Fluxnet: A new tool to study the temporal and spatial variability of ecosystem-scale carbon dioxide, water vapor, and energy flux densities, Bulletin of the American Meteorological Society, 82, 2415-2434, 10.1175/1520-0477(2001)082<2415:fantts>2.3.co;2, 2001.

Baldocchi, D.: Breathing of the terrestrial biosphere: Lessons learned from a global network of carbon dioxide flux measurement systems, Australian Journal of Botany, 56, 1-26, 10.1071/bt07151, 2008.

Barlow, J. F., Dunbar, T. M., Nemitz, E. G., Wood, C. R., Gallagher, M. W., Davies, F., O'Connor, E., and Harrison, R. M.: Boundary layer dynamics over London, UK, as observed using Doppler LIDAR during REPARTEE-II, Atmospheric Chemistry and Physics, 11, 2111-2125, 10.5194/acp-11-2111-2011, 2011.

Barlow, J. F., Halios, C. H., Lane, S. E., and Wood, C. R.: Observations of urban boundary layer structure during a strong urban heat island event, Environmental Fluid Mechanics, 15, 373-398, 10.1007/s10652-014-9335-6, 2015.

Bjorkegren, A. B., Grimmond, C. S. B., Kotthaus, S., and Malamud, B. D.: $CO_2$ emission estimation in the urban environment: Measurement of the $CO_2$ storage term, Atmospheric Environment, 122, 775-790, http://dx.doi.org/10.1016/j.atmosenv.2015.10.012, 2015.

Bohnenstengel, S. I., Belcher, S. E., Aiken, A., Allan, J. D., Allen, G., Bacak, A., Bannan, T. J., Barlow, J. F., Beddows, D. C. S., Bloss, W. J., Booth, A. M., Chemel, C., Coceal, O., Di Marco, C. F., Dubey, M. K., Faloon, K. H., Fleming, Z. L., Furger, M., Gietl, J. K., Graves, R. R., Green, D. C., Grimmond, C. S. B., Halios, C. H., Hamilton, J. F., Harrison, R. M., Heal,

M. R., Heard, D. E., Helfter, C., Herndon, S. C., Holmes, R. E., Hopkins, J. R., Jones, A. M., Kelly, F. J., Kotthaus, S., Langford, B., Lee, J. D., Leigh, R. J., Lewis, A. C., Lidster, R. T., Lopez-Hilfiker, F. D., McQuaid, J. B., Mohr, C., Monks, P. S., Nemitz, E., Ng, N. L., Percival, C. J., Prevot, A. S. H., Ricketts, H. M. A., Sokhi, R., Stone, D., Thornton, J. A., Tremper, A. H., Valach, A. C., Visser, S., Whalley, L. K., Williams, L. R., Xu, L., Young, D. E., and Zotter, P.: Meteorology, air quality, and health in London the ClearfLo project, Bulletin of the American Meteorological Society, 96, 779-804, 10.1175/bams-d-12-00245.1, 2015.

Cambaliza M.O.L., S. P., Bogner J., Caulton D.R., Stirm B., et al.: Quantification and source apportionment of the methane emission flux from the city of Indianapolis., Elementa Science of the Anthropocene, 3, 10.12952/journal.elementa.000037, 2015.

Carslaw, D. C. and Ropkins K.: openair --- an R package for air quality data analysis. Environmental Modelling & Software. Volume 27-28, 52-61, 2012.

Carslaw D.C. and Ropkins K.: openair: Open-source tools for the analysis of air pollution data. R package version 1.7-3, http://CRAN.R-project.org/package=openair, 2016.

Christen, A., Coops, N. C., Crawford, B. R., Kellett, R., Liss, K. N., Olchovski, I., Tooke, T. R., van der Laan, M., and Voogt, J. A.: Validation of modeled carbon-dioxide emissions from an urban neighborhood with direct eddy-covariance measurements, Atmospheric Environment, 45, 6057-6069, 10.1016/j.atmosenv.2011.07.040, 2011.

Christen, A.: Atmospheric measurement techniques to quantify greenhouse gas emissions from cities, Urban Climate, 10, Part 2, 241-260, http://dx.doi.org/10.1016/j.uclim.2014.04.006, 2014.

Crosson, E. R.: A cavity ring-down analyzer for measuring atmospheric levels of methane, carbon dioxide, and water vapor, Applied Physics B-Lasers and Optics, 92, 403-408, 10.1007/s00340-008-3135-y, 2008.

Evans, S.: 3D cities and numerical weather prediction models: An overview of the methods used in the LUCID project, available at http://discovery.Ucl.Ac.Uk/17404/1/17404.Pdf UCL Working Paper Series, 2009.

Fiddler, M. N., Begashaw, I., Mickens, M. A., Collingwood, M. S., Assefa, Z., and Bililign, S.: Laser spectroscopy for atmospheric and environmental sensing, Sensors, 9, 10447-10512, 10.3390/s91210447, 2009.

Finkelstein, P. L., and Sims, P. F.: Sampling error in eddy correlation flux measurements, Journal of Geophysical Research: Atmospheres, 106, 3503-3509, 10.1029/2000jd900731, 2001.

Foken, T., and Wichura, B.: Tools for quality assessment of surface-based flux measurements, Agricultural and Forest Meteorology, 78, 83-105, 10.1016/0168-1923(95)02248-1, 1996.

Foken, T.: Micrometeorology, Springer-Verlag Berlin Heidelberg, 308 pp., 2008.

Foken, T., Gödecke, M., Mauder, M., Mahrt, L., Amiro, B., and Munger, W.: Post-field data quality control, in: Handbook of micrometeorology, edited by: Lee, X., Kluwer Academic Publishers, 2004.

Gioli, B., Toscano, P., Lugato, E., Matese, A., Miglietta, F., Zaldei, A., and Vaccari, F. P.: Methane and carbon dioxide fluxes and source partitioning in urban areas: The case study of Florence, Italy, Environmental Pollution, 164, 125-131, 10.1016/j.envpol.2012.01.019, 2012.

Greater London Authority**,** London Datastore: http://data.london.gov.uk/, 2016.

Grimmond, C. S. B., and Christen, A.: Flux measurements in urban ecosystems, in: FluxLetter, The newsletter of FLUXNET, 1, FLUXNET, 2012.

Halios, C. H., and Barlow, J. F.: Observations of the morning development of the urban boundary layer over London, UK, taken during the actual project. , Boundary-Layer Meteorology, under review 2016.

Harrison, R. M., Dall'Osto, M., Beddows, D. C. S., Thorpe, A. J., Bloss, W. J., Allan, J. D., Coe, H., Dorsey, J. R., Gallagher, M., Martin, C., Whitehead, J., Williams, P. I., Jones, R. L., Langridge, J. M., Benton, A. K., Ball, S. M., Langford, B., Hewitt, C. N., Davison, B., Martin, D., Petersson, K. F., Henshaw, S. J., White, I. R., Shallcross, D. E., Barlow, J. F., Dunbar, T., Davies, F., Nemitz, E., Phillips, G. J., Helfter, C., Di Marco, C. F., and Smith, S.: Atmospheric chemistry and physics in the atmosphere of a developed megacity (London): an overview of the REPARTEE experiment and its conclusions, Atmospheric Chemistry and Physics, 12, 3065-3114, 2012.

Helfter, C., Famulari, D., Phillips, G. J., Barlow, J. F., Wood, C. R., Grimmond, C. S. B., and Nemitz, E.: Controls of carbon dioxide concentrations and fluxes above central London, Atmospheric Chemistry and Physics, 11, 1913-1928, 10.5194/acp-11-1913-2011, 2011.

Hsu, Y.-K., VanCuren, T., Park, S., Jakober, C., Herner, J., FitzGibbon, M., Blake, D. R., and Parrish, D. D.: Methane emissions inventory verification in Southern California, Atmospheric Environment, 44, 1-7, 10.1016/j.atmosenv.2009.10.002, 2010.

International Energy Agency: World energy outlook, http://www.iea.org/publications/freepublications/publication/world-energy-outlook-2012.html, 2012.

IPCC (International Panel on Climate Change): IPCC fifth assessment report: Climate change 2013, 2013.

Jarvi, L., Nordbo, A., Junninen, H., Riikonen, A., Moilanen, J., Nikinmaa, E., and Vesala, T.: Seasonal and annual variation of carbon dioxide surface fluxes in Helsinki, Finland, in 2006-2010, Atmospheric Chemistry and Physics, 12, 8475-8489, 10.5194/acp-12-8475-2012, 2012.

Kormann, R., and Meixner, F. X.: An analytical footprint model for non-neutral stratification, Boundary-Layer Meteorology, 99, 207-224, 10.1023/a:1018991015119, 2001.

Kotthaus, S., and Grimmond, C. S. B.: Identification of micro-scale anthropogenic $CO_2$, heat and moisture sources - processing eddy covariance fluxes for a dense urban environment, Atmospheric Environment, 57, 301-316, 10.1016/j.atmosenv.2012.04.024, 2012.

Kotthaus, S., and Grimmond, C. S. B.: Energy exchange in a dense urban environment – part II: Impact of spatial heterogeneity of the surface, Urban Climate, 10, Part 2, 281-307, http://dx.doi.org/10.1016/j.uclim.2013.10.001, 2014a.

Kotthaus, S., and Grimmond, C. S. B.: Energy exchange in a dense urban environment – part I: Temporal variability of long-term observations in central London, Urban Climate, 10, Part 2, 261-280, http://dx.doi.org/10.1016/j.uclim.2013.10.002, 2014b.

Langford, B., Nemitz, E., House, E., Phillips, G. J., Famulari, D., Davison, B., Hopkins, J. R., Lewis, A. C., and Hewitt, C. N.: Fluxes and concentrations of volatile organic compounds above central London, UK, Atmospheric Chemistry and Physics, 10, 627-645, 10.5194/acp-10-627-2010, 2010.

Liu, H. Z., Feng, J. W., Jarvi, L., and Vesala, T.: Four-year (2006-2009) eddy covariance measurements of $CO_2$ flux over an urban area in Beijing, Atmospheric Chemistry and Physics, 12, 7881-7892, 10.5194/acp-12-7881-2012, 2012.

Lowry, D., Holmes, C. W., Rata, N. D., O'Brien, P., and Nisbet, E. G.: London methane emissions: Use of diurnal changes in concentration and delta C-13 to identify urban sources and verify inventories, Journal of Geophysical Research-Atmospheres, 106, 7427-7448, 10.1029/2000jd900601, 2001.

McKain, K. K., Down, A., Raciti, S. M., Budney, J., Hutyra, L. R., Floerchinger, C., Herndon, S. C., Nehrkorn, T., Zahniser, M. S., Jackson, R. B., Phillips, N., and Wofsy, S. C.: Methane emissions from natural gas infrastructure and use in the urban region of Boston, Massachusetts, Proceedings of the National Academy of Sciences of the United States of America, 112, 1941-1946, 10.1073/pnas.1416261112, 2015.

Nam, E. K., Jensen, T. E., and Wallington, T. J.: Methane emissions from vehicles, Environmental Science & Technology, 38, 2005-2010, 10.1021/es034837g, 2004.

Moncrieff, J., Clement, R., Finnigan, J., and Meyers, T.: Averaging, detrending and filtering of eddy covariance time series. In: Handbook of Micrometeorology, Lee, X. (Ed.), Kluwer Academic Publishers, 2004.

O'Shea, S. J., Allen, G., Fleming, Z. L., Bauguitte, S. J. B., Percival, C. J., Gallagher, M. W., Lee, J., Helfter, C., and Nemitz, E.: Area fluxes of carbon dioxide, methane, and carbon monoxide derived from airborne measurements around greater London: A case study during summer 2012, Journal of Geophysical Research-Atmospheres, 119, 4940-4952, 10.1002/2013jd021269, 2014.

Mayor of London Office: London population confirmed at record high: https://www.london.gov.uk/media/mayor-press-releases/2015/02/london-population-confirmed-at-record-high, 2015.

Pawlak, W., Fortuniak, K., and Siedlecki, M.: Carbon dioxide flux in the centre of Lodz, Poland - analysis of a 2-year eddy covariance measurement data set, International Journal of Climatology, 31, 232-243, 10.1002/joc.2247, 2011.

Pawlak, W. and Fortuniak, K.: Eddy covariance measurements of the net turbulent methane flux in the city centre – results of 2 years campaign in Łódź, Poland, Atmos. Chem. Phys. Discuss., 2016, 1-38, 2016.

Peltola, O., Hensen, A., Helfter, C., Marchesini, L. B., Bosveld, F. C., van den Bulk, W. C. M., Elbers, J. A., Haapanala, S., Holst, J., Laurila, T., Lindroth, A., Nemitz, E., Rockmann, T., Vermeulen, A. T., and Mammarella, I.: Evaluating the performance of commonly used gas analysers for methane eddy covariance flux measurements: The InGOS inter-comparison field experiment, Biogeosciences, 11, 3163-3186, 10.5194/bg-11-3163-2014, 2014.

United Nations: World urbanization prospects, http://esa.un.org/unpd/wup/highlights/wup2014-highlights.pdf, 2014.

Ward, H. C., Kotthaus, S., Grimmond, C. S. B., Bjorkegren, A., Wilkinson, M., Morrison, W. T. J., Evans, J. G., Morison, J. I. L., and Iamarino, M.: Effects of urban density on carbon dioxide exchanges: Observations of dense urban, suburban and woodland areas of southern England, Environmental Pollution, 198, 186-200, 10.1016/j.envpol.2014.12.031, 2015.

Wennberg, P. O., Mui, W., Wunch, D., Kort, E. A., Blake, D. R., Atlas, E. L., Santoni, G. W., Wofsy, S. C., Diskin, G. S., Jeong, S., and Fischer, M. L.: On the sources of methane to the Los Angeles atmosphere, Environmental Science & Technology, 46, 9282-9289, 10.1021/es301138y, 2012.

Wood, C. R., Lacser, A., Barlow, J. F., Padhra, A., Belcher, S. E., Nemitz, E., Helfter, C., Famulari, D., and Grimmond, C. S. B.: Turbulent flow at 190 m height above London during 2006-2008: A climatology and the applicability of similarity theory, Boundary-Layer Meteorology, 137, 77-96, 10.1007/s10546-010-9516-x, 2010.

Wunch, D., Wennberg, P. O., Toon, G. C., Keppel-Aleks, G., and Yavin, Y. G.: Emissions of greenhouse gases from a North American megacity, Geophysical Research Letters, 36, 10.1029/2009gl039825, 2009.

Zazzeri, G., Lowry, D., Fisher, R. E., France, J. L., Lanoiselle, M., and Nisbet, E. G.: Plume mapping and isotopic characterisation of anthropogenic methane sources, Atmospheric Environment, 110, 151-162, 10.1016/j.atmosenv.2015.03.029, 2015.

## Tables

**Table 1: Annual totals of carbon dioxide flux and methane flux calculated from monthly averages for the period 2012-2014. The data period September 2012-March 2013 (no ultrasonic anemometer) was gapfilled using available monthly averages obtained over the remaining measurement period. Due to insufficient temporal coverage, individual annual budgets for 2012-2014 could not be derived for the carbon monoxide flux. A composite annual emissions estimate was compiled instead which makes use of all available monthly averages of $F_{CO}$ over the study period September 2011 to December 2014. Data from the London Atmospheric Emissions Inventory (LAEI; emissions for the central London boroughs of Westminster and Camden) and previous measurement campaigns are provided for comparison with the current study.**

| | Reference | $FCO_2$ [kt km$^{-2}$] | $FCH_4$ [t km$^{-2}$] | FCO [t km$^{-2}$] |
|---|---|---|---|---|
| **2012** | This study | 40.2 | 69 | - |
| **2013** | This study | 40.7 | 75 | - |
| **2014** | This study | 36.3 | 72 | - |
| **Mean ± SD** | This study | 39.1 ± 2.4 | 72 ± 3 | 89 |
| **Random uncertainty** | This study | 6.5 | 12 | 16 |
| **Emissions inventory (2012)** | LAEI | 38.7 | 29 | 110 |
| **London 2007** | (Helfter et al., 2011) | 35.5 | - | - |
| **London** | (Ward et al., 2015) | 46.6 | | |
| **London Autumn 2007/08** | (Harrison et al., 2012) | | | 150 - 220 |
| **London July 2012** | (O'Shea et al., 2014) ǂ | 29.0 | 66 | 106 |

ǂ **Aircraft measurements.**

**Table 2: Emission ratios from measurements and the London Atmospheric Emissions Inventory (LAEI). Measured quantities are mean, median and range of monthly emissions segregated by wind direction.**

| Emission category | Zone | $F_{CH4}/F_{CO2}$ | $F_{CO}/F_{CO2}$ | $F_{CO}/F_{CH4}$ |
|---|---|---|---|---|
| **Measured (this study):** | | | | |
| Mean | | 0.0019 | 0.0018 | 0.9739 |
| Median | | 0.0019 | 0.0021 | 1.1304 |
| Minimum | | 0.0017 | 0.0004 | 0.1972 |
| Maximum | | 0.0022 | 0.0027 | 1.5951 |
| **LAEI (all sources)** | Central | 0.0009 | 0.0039 | 4.1023 |
| | Inner | 0.0010 | 0.0024 | 2.4546 |
| | Outer | 0.0094 | 0.0018 | 0.1965 |
| **Domestic Coal** | Central | - | - | - |
| | Inner | 0.0020 | 0.0460 | 22.400 |
| | Outer | 0.0020 | 0.0460 | 22.414 |
| **Domestic Oil** | Everywhere | 0.0001 | 0.0006 | 4.0000 |
| **Domestic Gas** | Everywhere | 0.0001 | 0.0006 | 6.0375 |
| **Non-Domestic Gas** | Everywhere | 0.0001 | 0.0002 | 2.2642 |
| **Boilers** | Central | 0.0001 | 4E-05 | 0.3270 |
| | Inner | 0.0001 | 5E-05 | 0.3548 |
| | Outer | 0.0001 | 5E-05 | 0.3482 |
| **Gas Leakage** | Everywhere | 26.607 | - | - |
| **Non-Road Mobile Machinery, agriculture & other** | Central | 0.0002 | 0.0347 | 213.55 |
| | Inner | 0.0003 | 0.0377 | 119.75 |
| | Outer | 0.3525 | 0.0576 | 0.1633 |
| **Road - All Sources** | Central | - | 0.0021 | - |
| | Inner | - | 0.0013 | - |
| | Outer | - | 0.0013 | - |

**Table 3: Goodness of fit of the linear regression between wind sector-segregated monthly methane fluxes ($F_{CH4}$), carbon dioxide fluxes ($F_{CO2}$) and monthly mean air temperature ($T_{air}$). The superscripts (-) and (+) denote the sign of slope for each linear regression. P-values in bold denote statistical significance.**

| $R^2$ | N | NE | E | SE | S | SW | W | NW |
|---|---|---|---|---|---|---|---|---|
| **$F_{CH4}$ v. $T_{air}$** | $0.55^{(-)}$ | $0.43^{(-)}$ | $0.73^{(-)}$ | $0.08^{(-)}$ | $0.04^{(-)}$ | $0.05^{(-)}$ | $0.60^{(-)}$ | $0.21^{(-)}$ |
| **p-value** | **0.0060** | **0.0197** | **0.0004** | 0.3627 | 0.5150 | 0.4790 | **0.0033** | 0.1367 |
| **$F_{CO2}$ v. $T_{air}$** | **$0.51^{(-)}$** | **$0.69^{(-)}$** | **$0.80^{(-)}$** | $0.19^{(-)}$ | $0.18^{(-)}$ | $0.27^{(-)}$ | **$0.60^{(-)}$** | $0.34^{(-)}$ |
| **p-value** | **0.0203** | **0.0021** | **0.0003** | 0.1496 | 0.1984 | 0.1650 | **0.0081** | 0.0776 |

## Figures

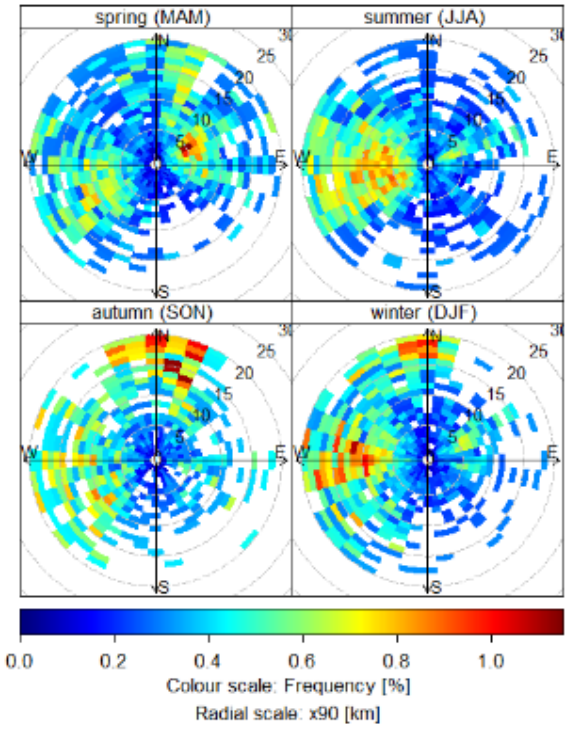


**Figure 1: Frequency of occurrence of $x_{90}$ (distance from the tower where 90% of the measured fluxes originated from) centred at the BT tower as a function of wind direction and season. The flux footprint was estimated using an analytical model for non-neutral stratification (Kormann and Meixner, 2001) and the plots were produced using the openair package for R (Carslaw and Ropkins, 2012; Carslaw and Ropkins, 2016). Bin dimensions: 10° (angular scale) × 1 km (radial scale). Data period 15/09/2011-31/12/2014.**

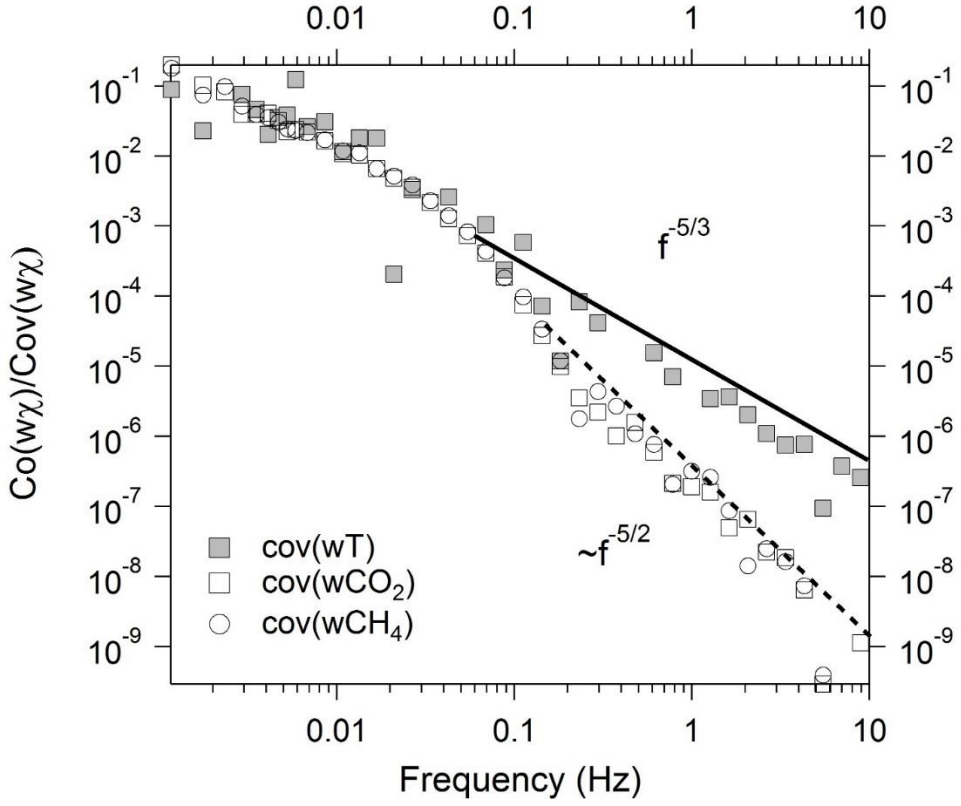


**Figure 2: Normalised cospectra of T (sonic temperature), $CO_2$ and $CH_4$ with respect to w (vertical wind component). Each cospectrum is an average of 24 half-hourly cospectra (data period 12/03/2013 7:00 – 18:00). Regression of spectra for frequencies > 0.1 Hz marked by solid line for Co(wT) and dashed line for both Co(w$CO_2$) and Co(w$CH_4$).**

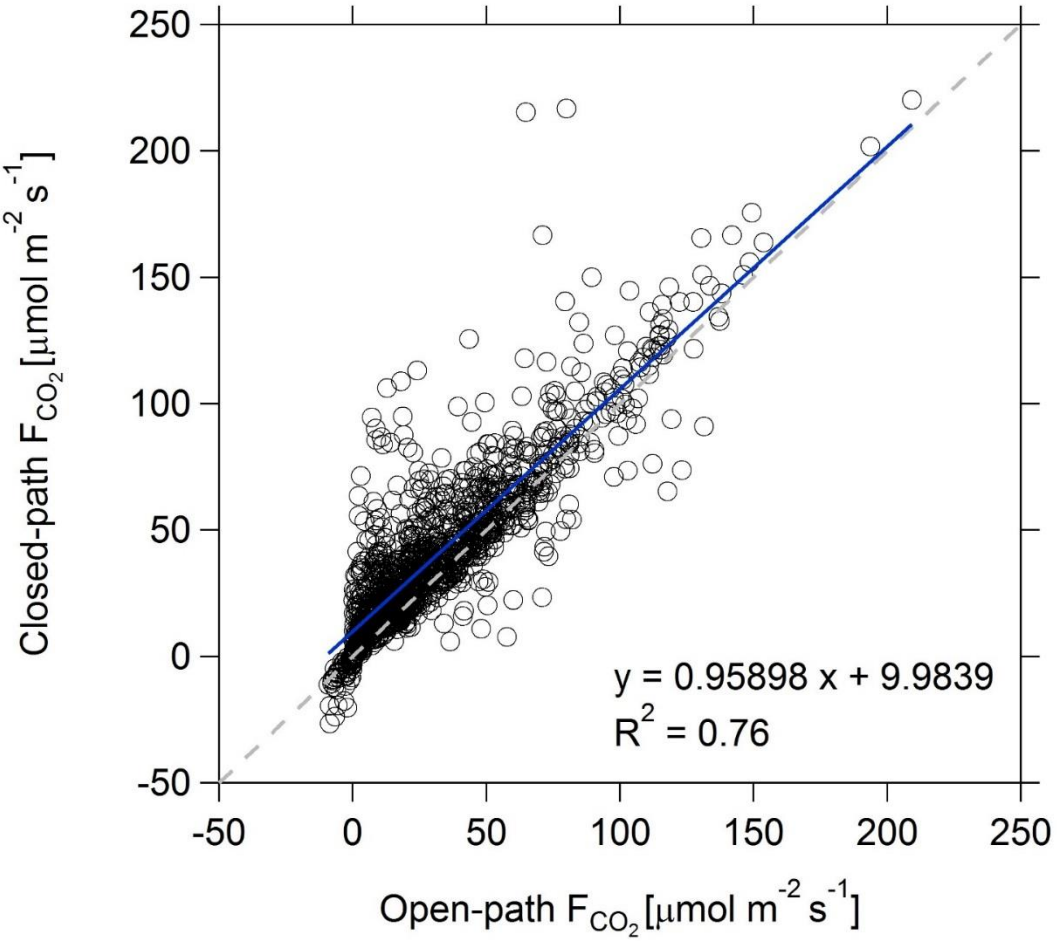


**Figure 3: Comparison of half-hourly fluxes of $CO_2$ measured in March, August and October 2013 by a closed-path Picarro G1301-f operating at 1 Hz following high-frequency loss correction and an open-path Li7500 analyser operating at 20 Hz at the top of BT tower (sensor height: 190 m a.g.l.). Dashed line is 1:1 line.**

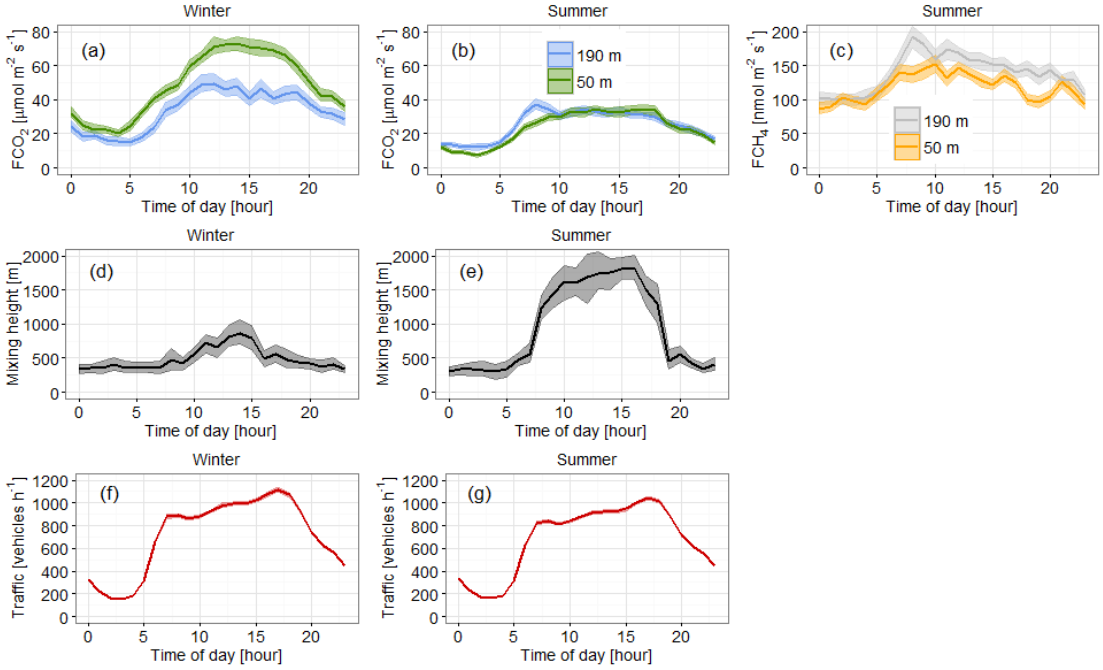


**Figure 4: Mean diurnal profiles of $CO_2$ fluxes for (a) winter (DJF), and (b) summer (JJA) for the data period 15/09/2011 – 31/12/2013; (c) $CH_4$ fluxes in summer observed at the BT tower site (190 m a.g.l.) and the KCL site (50 m a.g.l.) over the period 19/08 – 01/10/2015; mixing height obtained from Doppler LIDAR measurements for (d) winter and (e) summer (Bohnenstengel et al., 2015); road traffic counts (f) winter and (g) summer (average of 246 counting stations distributed throughout the London conurbation; source: Transport for London, 2012 data). The shaded areas represent the 95% confidence interval.**

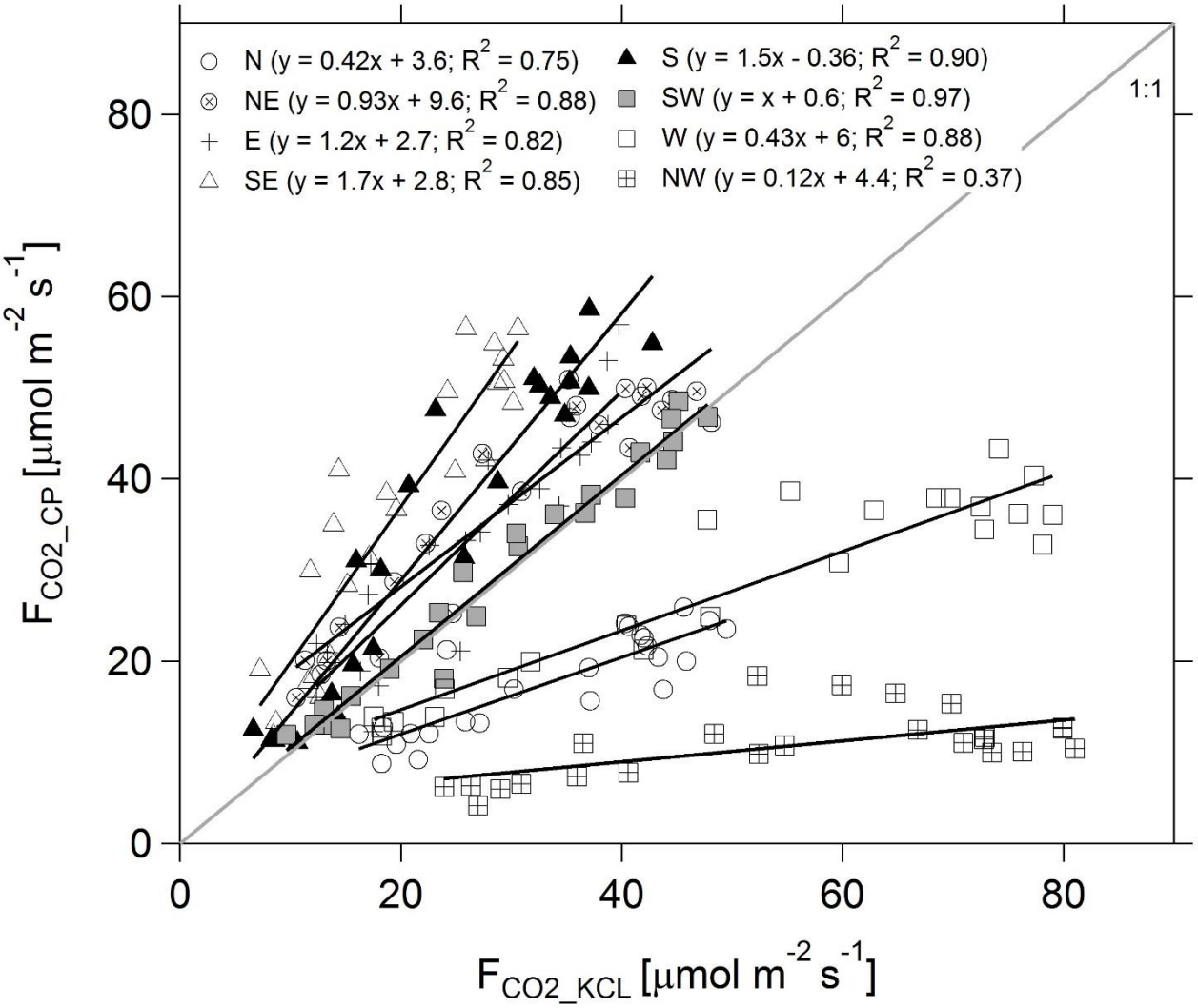


**Figure 5: Comparison between average diurnal profiles of $CO_2$ fluxes measured at the BT tower (190 m a.g.l.) and at the KCL site (50 m a.g.l.) in the period 15/09/2011 – 31/12/2013, separated into eight wind-direction sectors based on the wind direction observed at BT tower.**

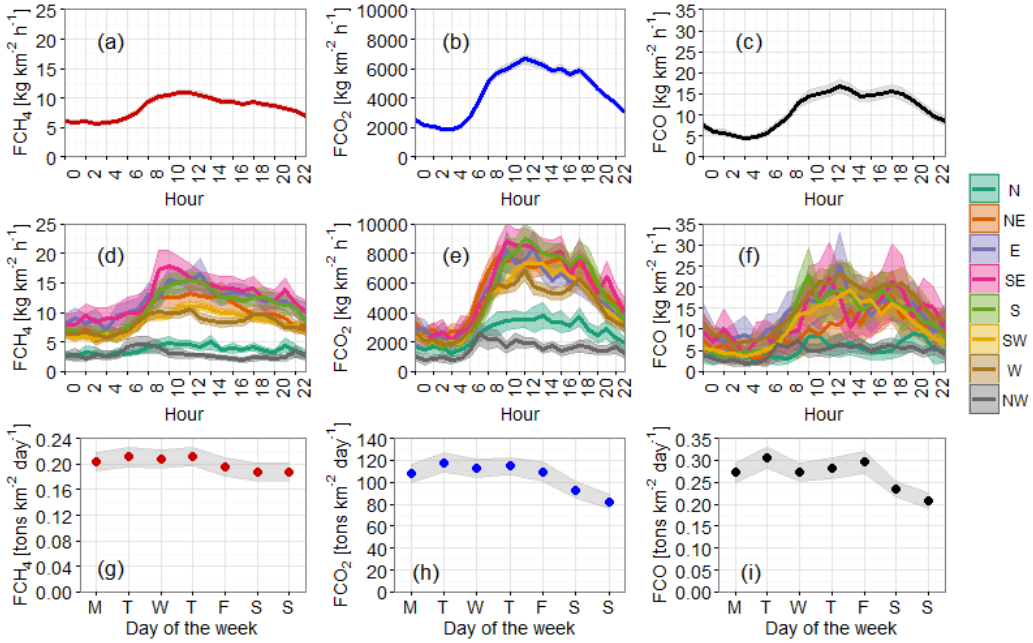


**Figure 6: Fluxes of (a, d, g) methane ($F_{CH4}$), (b, e, h) carbon dioxide ($F_{CO2}$) and (c, f, i) carbon monoxide ($F_{CO}$) observed at BT tower with a closed-path gas analyser (from 15/09/2011 to 31/12/2014): (a)-(c) mean diurnal patterns with 95% confidence interval (shading), (d)-(f) as (a)-(c) but segregated into wind sectors and (g)-(i) by day of the week.**

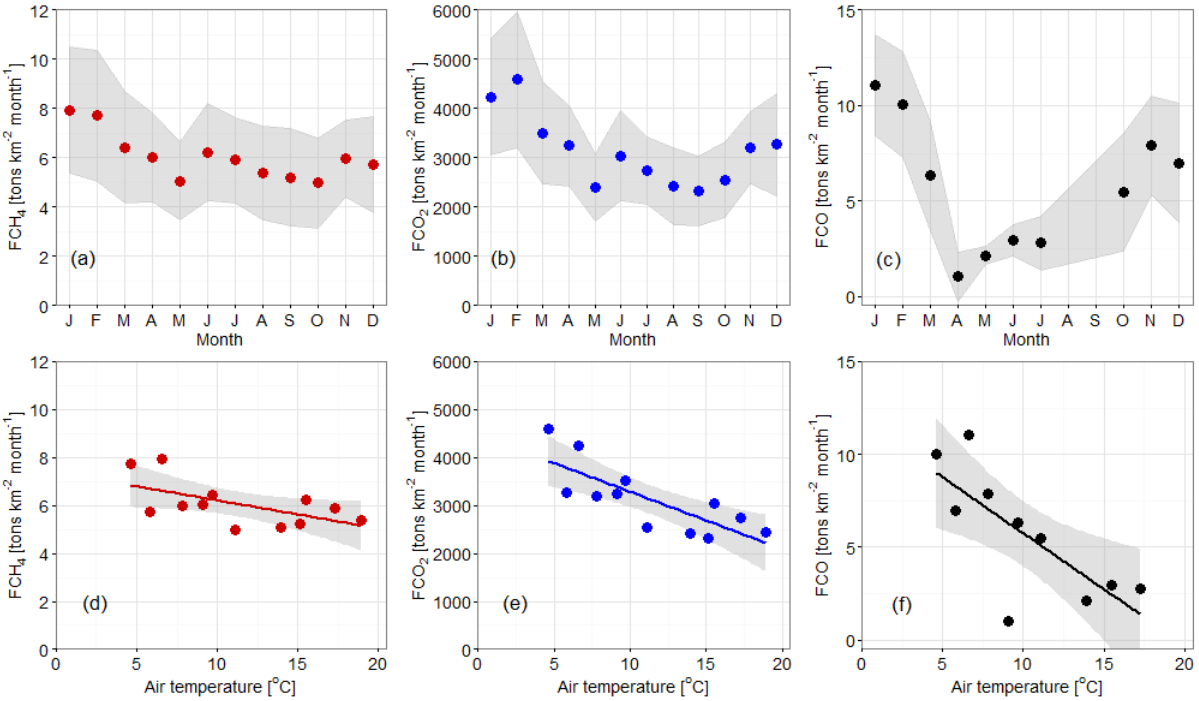


**Figure 7: (a)-(c): Monthly averages of $F_{CH4}$, $F_{CO2}$ and $F_{CO}$ (September 2011-December 2014); (d)-(f): $F_{CH4}$, $F_{CO2}$ and $F_{CO}$ as a function of monthly mean air temperature. Solid lines are linear regressions and shaded areas are 95% confidence intervals. No $F_{CO}$ measurements were available in August and September due to instrument downtime.**

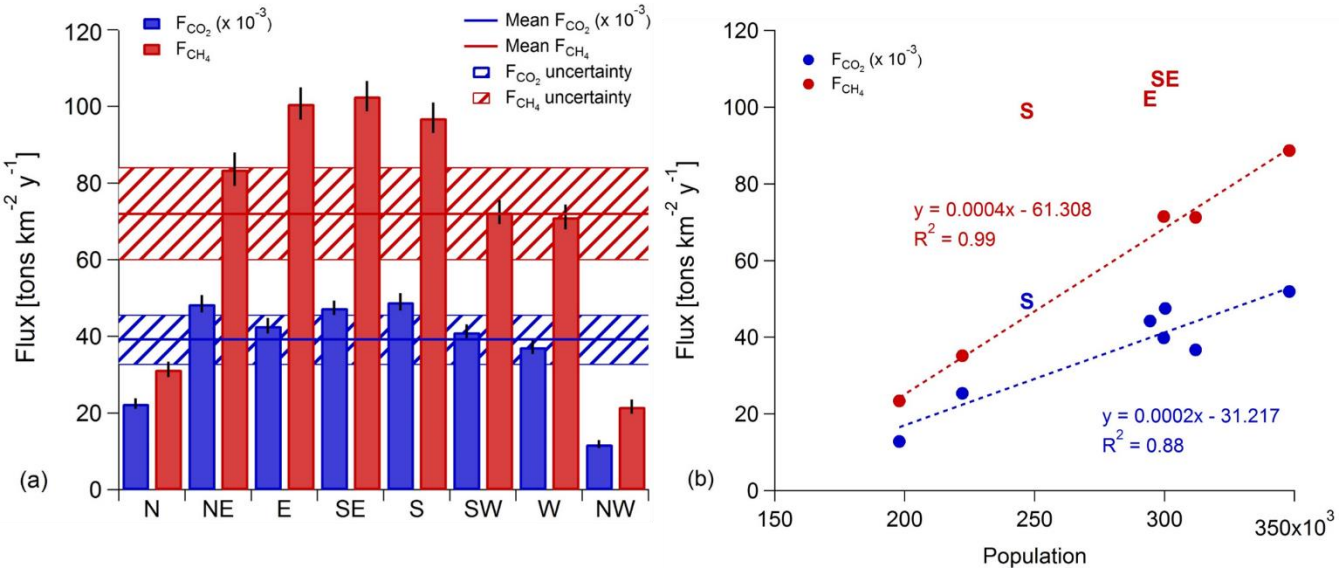


**Figure 8: Annual fluxes of carbon dioxide ($F_{CO2}$) and methane ($F_{CH4}$) measured by eddy-covariance at the BT tower in central London as a function of (a) wind direction; solid lines are mean annual emissions (2012-2014) without wind sector segregation. Measurement uncertainty (taken as the maximum of monthly uncertainties for each gas) is denoted by a blue ($F_{CO2}$) and red striped areas ($F_{CH4}$). (b) Data from plot (a) as a function of population within each wind sector-specific flux footprint area. The spatial extent of the footprint for each wind sector was derived from footprint statistics (Fig. 1) with the approximation that the typical extent was of the order of 10 km for NE-SW and 15 km for W-N. Population data (source: London Datastore, Greater London Authority, 2016) are on a ward basis (i.e. sub-borough administrative unit). Linear regression (dashed lines), with exclusion of S sector data point for $F_{CO2}$, E, S and SE for $F_{CH4}$ (identified by their wind sector abbreviations). NB: $F_{CO2}$ and associated uncertainty are divided by 1000 to aid visualisation.**